Hindawi Publishing Corporation
Advances in High Energy Physics
Volume 2012, Article ID 462493, 12 pages
doi:10.1155/2012/462493

Research Article

On the Stability of Thin-Shell Wormholes in Noncommutative Geometry

Peter K. F. Kuhfittig

Department of Mathematics, Milwaukee School of Engineering, Milwaukee, WI 53202-3109, USA

Correspondence should be addressed to Peter K. F. Kuhfittig, kuhfitti@msoe.edu

Received 2 February 2012; Revised 15 April 2012; Accepted 24 April 2012

Academic Editor: George Siopsis

This paper reexamines a special class of thin-shell wormholes that are unstable in general relativity in the framework of noncommutative geometry. It is shown that, as a consequence of the intrinsic uncertainty, these wormholes are stable to small linearized radial perturbations. Several different spacetimes are considered.

1. Introduction

An important outcome of string theory is the realization that coordinates may become noncommuting operators on a D-brane [1, 2]. The result is a fundamental discretization of spacetime due to the commutator $[\mathbf{x}^\mu, \mathbf{x}^\nu] = i\theta^{\mu\nu}$, where $\theta^{\mu\nu}$ is an antisymmetric matrix, in much the same way as the Planck constant $\hbar$ discretizes phase space [3]. Moreover, noncommutativity is an intrinsic property of spacetime and does not depend on particular features such as curvature.

It was pointed out by Smailagic and Spallucci [4] that noncommutativity replaces point-like structures by smeared objects and so may eliminate the divergences that normally appear in general relativity. An effective way to model the smearing effect is by the use of the Gaussian distribution of minimal length $\sqrt{\alpha}$ instead of the Dirac-delta function. As a result, according to Nicolini et al. [5], the energy density of the static and spherically symmetric smeared and particle-like gravitational source has the form

$$\rho(r) = \frac{m}{(4\pi\alpha)^{3/2}} e^{-r^2/4\alpha}, \tag{1.1}$$

that is, the mass m is diffused throughout the region of linear dimension $\sqrt{\alpha}$ due to the uncertainty. Using this gravitational source in the Einstein field equations, the line element was found to be

$$ds^2 = -\left(1 - \frac{2m^*(r)}{r}\right)dt^2 + \frac{dr^2}{1 - 2m^*(r)/r} + r^2\left(d\theta^2 + \sin^2\theta\, d\phi^2\right), \tag{1.2}$$

where

$$m^*(r) = \frac{2m}{\sqrt{\pi}}\gamma\left(\frac{3}{2}, \frac{r^2}{4\alpha}\right) = \frac{2m}{\sqrt{\pi}}\int_0^{r^2/4\alpha} \sqrt{t}e^{-t}dt. \tag{1.3}$$

Here,

$$\gamma\left(\frac{3}{2}, \frac{r^2}{4\alpha}\right) = \int_0^{r^2/4\alpha} \sqrt{t}e^{-t}dt \tag{1.4}$$

is the lower incomplete gamma function. The classical Schwarzschild mass is recovered in the limit as $r\sqrt{\alpha} \to \infty$. (Recall that the lower incomplete gamma function starts at the origin, rises sharply, and then approaches unity asymptotically.)

Some modification will be required when applying these ideas to thin-shell wormholes, discussed in the next section. For now, we need only to note that the throat is assumed to be a thin shell, a sphere of radius $r = a_0$. So instead of a smeared particle, we have a smeared surface.

The main purpose of this paper is to show that the special thin-shell wormholes discussed here are stable to small linearized radial perturbations given a noncommutative-geometry framework, even though they are unstable in the framework of classical general relativity (GR). For this reason, the concentration will be on the smeared spherical surface of radius a_0 rather than on smeared point-like structures, since the surface is directly affected by radial perturbations.

2. Thin-Shell Wormholes

A powerful theoretical method for constructing a class of spherically symmetric wormholes from black-hole spacetimes was proposed by Visser [6]. The starting point is a spherically symmetric line element

$$ds^2 = -f(r)dt^2 + \left[f(r)\right]^{-1}dr^2 + r^2\left(d\theta^2 + \sin^2\theta d\phi^2\right) \tag{2.1}$$

describing a black-hole spacetime. The construction begins with two copies of a black hole and removing from each the four-dimensional region

$$\Omega^{\pm} = \{r \leq a \mid a > r_h\}, \tag{2.2}$$

where $r = r_h$ is the (outer) event horizon. The topological identification of the timelike hypersurfaces

$$\partial\Omega^{\pm} = \{r = a \mid a > r_h\} \tag{2.3}$$

results in a manifold that is geodesically complete and possesses two asymptotically flat regions connected by a throat.

A dynamic analysis depends on the Lanczos equations and is now considered standard (see, e.g., [7–11])

$$S^i{}_j = -\frac{1}{8\pi}\left(\left[K^i{}_j\right] - \delta^i{}_j[K]\right), \tag{2.4}$$

where $[K_{ij}] = K^+_{ij} - K^-_{ij}$ and $[K]$ is the trace of $K^i{}_j$. In terms of the surface energy density σ and the surface pressure $\mathcal{P}$, $S^i{}_j = \text{diag}(-\sigma, \mathcal{P}, \mathcal{P})$. By letting $r = a$ be a function of time, it is shown by Poisson and Visser [9] that

$$\sigma = -\frac{1}{2\pi a}\sqrt{f(a) + \dot{a}^2}, \tag{2.5}$$

$$\mathcal{P} = -\frac{1}{2}\sigma + \frac{1}{8\pi}\frac{2\ddot{a} + f'(a)}{\sqrt{f(a) + \dot{a}^2}}. \tag{2.6}$$

(The overdot denotes the derivatives with respect to τ.) Since σ is negative on the sphere, we are dealing with exotic matter. Moreover, since the radial pressure p is zero for a thin shell, the weak energy condition is obviously violated.

3. Thin-Shell Wormholes with a Phantom-Like Equation of State

3.1. *In General Relativity*

As noted in the Introduction, we are going to be concerned with a special type of thin-shell wormholes, analyzed by Kuhfittig [12]. They are characterized by having a "phantom-like" equation of state $\mathcal{P} = \omega\sigma$, $\omega < 0$, on the shell, a natural analogue of the Chaplygin-gas equation of state used by Eiroa [7].

On the question of stability to linearized radial perturbations, we assume, as always, that $r = a$ is a function of time. It it readily checked that

$$\frac{d}{d\tau}\left(\sigma a^2\right) + \mathcal{P}\frac{d}{d\tau}\left(a^2\right) = 0 \tag{3.1}$$

which can also be written as

$$\frac{d\sigma}{da} + \frac{2}{a}(\sigma + \mathcal{P}) = 0. \tag{3.2}$$

For a static configuration of radius a_0, we have $\dot{a} = 0$ and $\ddot{a} = 0$. Given the equation of state $\mathcal{P} = \omega\sigma$, (3.2) can be solved by separation of variables to yield

$$\sigma(a) = \sigma_0\left(\frac{a_0}{a}\right)^{2(\omega+1)}, \quad \sigma_0 = \sigma(a_0). \tag{3.3}$$

Rearranging (2.5), we obtain the equation of motion

$$\dot{a}^2 + V(a) = 0. \tag{3.4}$$

Here, the potential $V(a)$ is defined as

$$V(a) = f(a) - [2\pi a\sigma(a)]^2. \tag{3.5}$$

Expanding $V(a)$ around a_0, we get

$$V(a) = V(a_0) + V'(a_0)(a - a_0) + \frac{1}{2}V''(a_0)(a - a_0)^2 + \mathcal{O}\Big[(a - a_0)^3\Big]. \tag{3.6}$$

Since we are linearizing around $a = a_0$, we require that $V(a_0) = 0$ and $V'(a_0) = 0$. The configuration is in stable equilibrium if $V''(a_0) > 0$.

3.2. In Noncommutative Geometry

A discussion of thin-shell wormholes in noncommutative geometry has to take into account the nature of the thin shell. The reason is that we are now dealing with a surface rather than a point-like structure. Moreover, we would expect the surface to be smeared as a consequence of the intrinsic uncertainty. So, returning to (1.3), observe that if a particle is located on the sphere $r = a_0$, then its mass is given by

$$m\int_0^{(r-a_0)^2/4\alpha} \frac{2}{\sqrt{\pi}}\sqrt{t}e^{-t}dt. \tag{3.7}$$

Here,

$$\gamma\left(\frac{3}{2}, \frac{(r-a_0)^2}{4\alpha}\right) = \int_0^{(r-a_0)^2/4\alpha} \sqrt{t}e^{-t}dt \tag{3.8}$$

is the corresponding lower incomplete gamma function, a pure translation of (1.4) by a distance $r = a_0$ in the r-direction, that is, independent of θ and ϕ, as shown, for example, by Rahaman et al. [13]. To visualize the process, one can simply choose a ray in a particular direction: now, the function starts at $r = a_0$ instead of the origin and approaches m asymptotically along the ray. The concentration on the radial direction is appropriate because we are interested in linearized radial perturbations.

The distance to a smeared object is necessarily smeared. Given the nature of the smearing in noncommutative geometry, we may assume that a smeared distance is proportional to the lower incomplete gamma function. The reason for this can also be seen from the following heuristic argument. Consider $m^*(r_0)$ for some arbitrary fixed r_0. Then, the proper distance ℓ between two points is from line element (1.2):

$$\ell = \int_a^b \frac{dr}{\sqrt{1-2m^*(r_0)/r}} = m^*(r_0)\int_a^b \frac{dr}{m^*(r_0)\sqrt{1-2m^*(r_0)/r}}, \tag{3.9}$$

which is indeed proportional to $\gamma(3/2, r_0^2/4\alpha)$. Now, $r \approx r_0$ for any small interval I containing r_0, so that, for all practical purposes, ℓ is proportional to $\gamma(3/2, r^2/4\alpha)$ on this interval. As a result, the smeared portion of the radius, which is necessarily small, is proportional to

$$a_0 \int_0^{(r-a_0)^2/4\alpha} \frac{2}{\sqrt{\pi}}\sqrt{t}e^{-t}dt, \quad r \geq a_0. \tag{3.10}$$

(Based on the expression for ℓ, the constant of proportionality would not be the same for every a_0. However, in the qualitative discussion below, the constant of proportionality has no bearing on the outcome and can therefore be taken as unity for any particular a_0.) For this interpretation to make sense, we have to treat m as a constant, just as a_0 is treated as a constant in (3.7). This is not a new assumption: even (1.3) assumes, unavoidably, a fixed position at $r = 0$.

One can argue that, in noncommutative geometry, any measured quantity will entail a degree of uncertainty. Since the stability question centers around the effect of a radial perturbation on the shell, we need to compare this effect on the two types of surfaces, smeared and unsmeared. To do so, the values of the other measured quantities need not be known precisely, as we will see in the next section.

4. Schwarzschild Wormholes

Recall that, for a Schwarzschild spacetime, we have from line element (2.1) that $f(r) = 1 - 2M/r$. So by (3.5)

$$V(a) = 1 - \frac{2M}{a} - 4\pi^2 a^2\sigma^2 = 1 - \frac{2M}{a} - 4\pi^2 a^2\sigma_0^2\left(\frac{a_0}{a}\right)^{4+4\omega}, \tag{4.1}$$

making use of (3.3). From (2.5) with $\dot{a} = 0$,

$$\sigma_0 = -\frac{1}{2\pi a_0}\sqrt{1-\frac{2M}{a_0}}. \tag{4.2}$$

Hence,

$$V(a) = 1 - \frac{2M}{a} - \left(1-\frac{2M}{a_0}\right)\frac{a_0^{2+4\omega}}{a^{2+4\omega}}. \tag{4.3}$$

The first requirement $V(a_0) = 0$ is met, but not the second. From

$$V'(a_0) = \frac{2M}{a_0^2} - \left(1 - \frac{2M}{a_0}\right) a_0^{2+4\omega}(-2-4\omega)a_0^{-3-4\omega} = 0, \tag{4.4}$$

we obtain the condition

$$\omega = -\frac{1}{2}\frac{a_0/M - 1}{a_0/M - 2}. \tag{4.5}$$

Substituting in $V''(a)$ and simplifying, we obtain

$$V''(a_0) = \frac{2}{a_0^2}\frac{-1}{a_0/M - 2} > 0. \tag{4.6}$$

Since $a_0/M - 2$ must be greater than zero to avoid an event horizon, the last condition cannot be met. As a result, there are no stable solutions for the Schwarzschild case.

Because of its simplicity, (4.6) provides a convenient bridge to analyzing the smearing effect in noncommutative geometry, that is, the effect of having a smeared surface. From (3.10),

$$V''(r) = \frac{2}{a_0^2}\frac{-1}{(a_0/M)\int_0^{(r-a_0)^2/4\alpha}(2/\sqrt{\pi})\sqrt{t}e^{-t}dt - 2} > 0. \tag{4.7}$$

(The reason for the change in notation is that V'' is now a function of r in the neighborhood of $r = a_0$.) Condition (4.7) can be easily met if the smearing is substantial enough, especially if a_0/M is reasonably close to 2.

To allow a comparison to the more complicated forms discussed later, let us consider the plot of $V''(r)$ in the neighborhood of the shell. Even though we are primarily interested in the qualitative features, we need to choose some specific values for the parameters to obtain a plot. Suppose we arbitrarily choose $\alpha = 0.01$ and $a_0/M = 5$. (For the purpose of illustration, M is assumed to be equal to unity.) Being arbitrary choices, the fact that these parameters are smeared quantities is now irrelevant. (This is also born out in the graphs, as we will see shortly.) For later convenience, we will include $a_0^2/2$ on the left side: being a positive quantity, it cannot affect the sign of $V''(r)$ in (4.7). So we have

$$\left(\frac{a_0^2}{2}\right)V_1''(r) = \frac{-1}{(a_0/M)\int_0^{(r-a_0)^2/4\alpha}(2/\sqrt{\pi})\sqrt{t}e^{-t}dt - 2} > 0. \tag{4.8}$$

The plot, shown in Figure 1, assumes smearing in both the inward and outward radial directions.

Since we are dealing here with a pure translation,

$$\left(\frac{a_0^2}{2}\right)V_2''(r) = \frac{-1}{(a_0/M)\int_0^{r^2/4\alpha}(2/\sqrt{\pi})\sqrt{t}e^{-t}dt - 2} \tag{4.9}$$

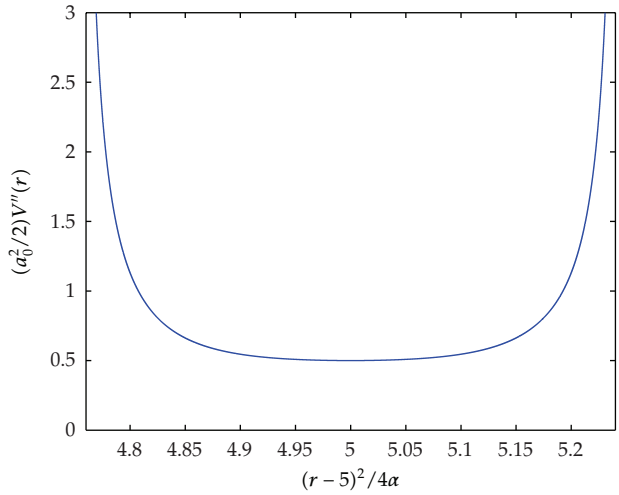

Figure 1: The Schwarzschild wormhole: $V'' > 0$ near $r = a_0$.

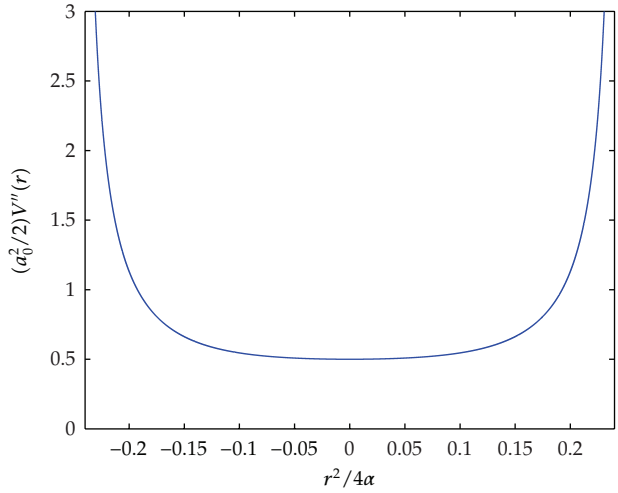

Figure 2: The graph of Figure 1 moved a_0 units to the left.

has exactly the same shape for the same α (Figure 2). So there is no need to translate $V''(r)$ to determine the effect of the smearing. The figures show that $V''(r)$ is positive around $r = a_0$, thereby yielding a small region of stability, that is, a small interval around $r = a_0$ where V(r) is concave up. As α gets closer to zero, the Gaussian curve (1.1), is reduced in width, so that the region of stability gets ever more narrow: Figure 3 shows $(a_0^2/2)V''(r)$ for $\alpha = 10^{-10}$. It is important to realize that the graph retains its basic shape regardless of the size of α or the size of a_0/M.

Remark 4.1. The invariance of the shape of the graphs shows even more clearly why, qualitatively speaking, the smearing of the parameters involved has no bearing on the stability analysis. Other parameters, such as σ and the pressure $\mathcal{P}$, do not come into play

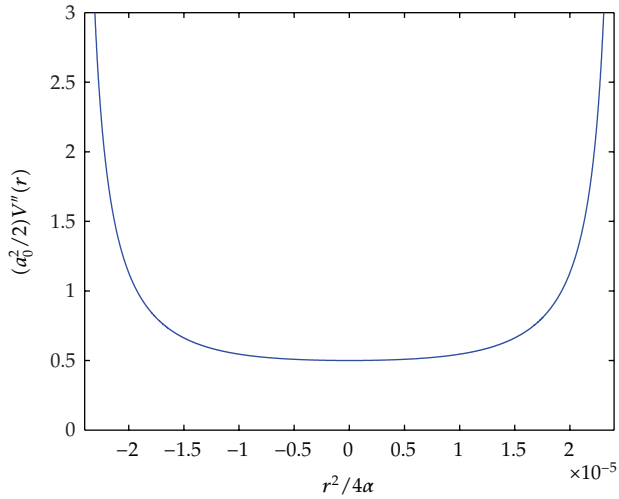

Figure 3: The Schwarzschild wormhole with $a_0/M = 5$ and $\alpha = 10^{-10}$. The region of stability is much reduced, implying that the wormhole is only stable to very small radial perturbations.

at all at this point, even though they are part of the dynamic analysis of the original shell $r = a$ in the GR case.

As a final comment, as α gets close to zero, the region of stability becomes vanishingly small, and the smaller the interval of concavity for V, the smaller the radial perturbations allowed.

Remark 4.2. Since the smearing effect is necessarily small, the most important applications may very well be found in the quantum regime: submicroscopic thin-shell wormholes with equation of state $\mathcal{P} = \omega\sigma$, $\omega < 0$, would be stable in a Schwarzschild spacetime.

5. Reissner-Nordström Wormholes

For a Reissner-Nordström spacetime, the starting point is

$$f(r) = 1 - \frac{2M}{r} + \frac{Q^2}{r^2}, \tag{5.1}$$

where M and Q are the mass and charge, respectively, of the black hole. If $0 < |Q| < M$, the black hole has two event horizons at $r = M \pm \sqrt{M^2 - Q^2}$ (and none if $|Q| > M$). Here, we have

$$V(a) = 1 - \frac{2M}{a} + \frac{Q^2}{a^2} - \left(1 - \frac{2M}{a_0} + \frac{Q^2}{a_0^2}\right)\left(\frac{a_0}{a}\right)^{2+4\omega}. \tag{5.2}$$

Once again, $V(a_0) = 0$. Following the same procedure discussed in the previous section, $V'(a_0) = 0$ yields ω and $V''(a_0)$ (see [12] for details). The result is

$$V''(a_0) = \frac{2}{a_0^2} \frac{-a_0/M - (Q^2/M^2)[1/(a_0/M)] + 2Q^2/M^2}{(a_0/M)^2 - 2a_0/M + Q^2/M^2} > 0. \tag{5.3}$$

As in the Schwarzschild case, V'' is a function of a_0; Q/M is fixed. It is also shown that, for a stable wormhole, we must have

$$\frac{|Q|}{M} > \frac{a_0/M}{\sqrt{2(a_0/M) - 1}}. \tag{5.4}$$

To meet this condition, $|Q|$ would have to exceed M. The result is a naked singularity for the black hole.

As before, since we now have a smeared surface, we replace a_0/M by

$$\left(\frac{a_0}{M}\right) \int_0^{r^2/4\alpha} \frac{2}{\sqrt{\pi}} \sqrt{t} e^{-t} dt. \tag{5.5}$$

(Recall that there is no need to translate the curve by replacing r by $r - a_0$.) We are primarily interested in a comparison to the GR case. So we retain Q/M as a fixed parameter, allowing us to concentrate on the smeared surface, which is subject to the radial perturbation.

Remark 5.1. As discussed in the previous section, in noncommutative geometry, all measured quantities entail a degree of uncertainty, including Q/M. The precise value is not needed, however, to draw the conclusion concerning stability, also reiterated next.

If we now arbitrarily let $a_0/M = 3$, then inequality (5.4) yields $Q > 1.34M$. To show that the wormhole has a stable region without requiring a naked singularity, we choose $Q/M = 1.2$ and $\alpha = 0.1$. Denoting the lower incomplete gamma function by γ, we plot

$$\left(\frac{a_0^2}{2}\right) V''(r) = \frac{-3\gamma - (1.2)^2 \cdot 1/3\gamma + 2(1.2)^2}{(3\gamma)^2 - 2(3)\gamma + (1.2)^2}. \tag{5.6}$$

The graph is shown in Figure 4. This time the interval is made wide enough to show that $V''(r)$ eventually becomes negative. As in the Schwarzschild case, a smaller α reduces the region of stability.

As another example, Figure 5 depicts the Reissner-Nordström case with $a_0/M = 12$, $Q/M = 0.5$, and $\alpha = 0.001$. As expected, the shape has remained similar.

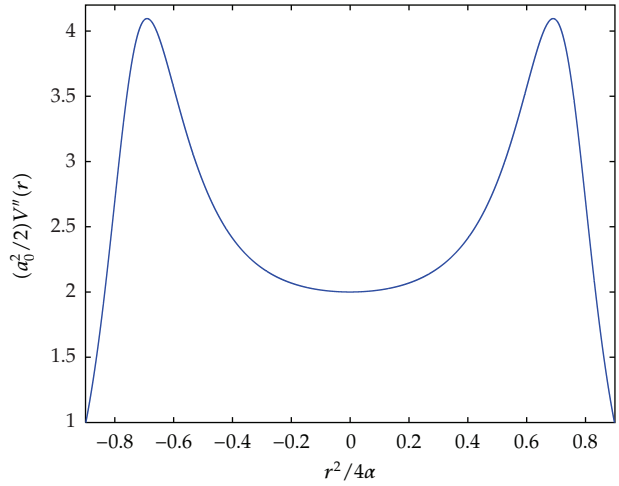

Figure 4: The Reissner-Nordström wormhole with $Q/M = 1.2$ and $\alpha = 0.1$, showing a region of stability without the need for a naked singularity.

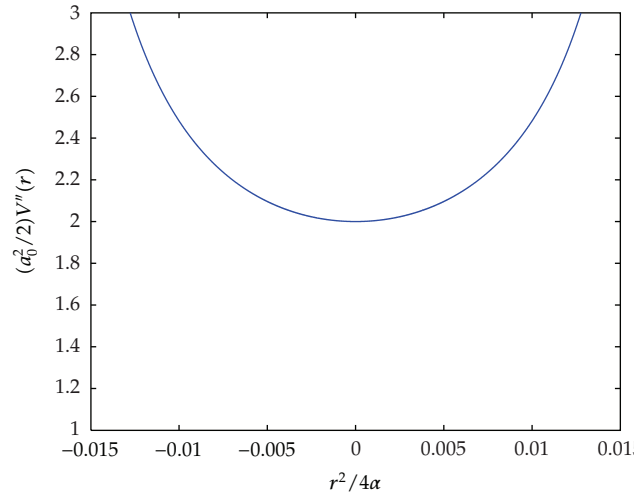

Figure 5: The Reissner-Nordström wormhole with $a_0/M = 12$, $Q/M = 0.5$, and $\alpha = 0.001$.

6. De Sitter and Anti-De Sitter Wormholes

In the presence of a cosmological constant, $f(r) = 1 - 2M/r - (1/3)\Lambda r^2$. For the de Sitter case, $\Lambda > 0$. To keep $f(r)$ from becoming negative, $\Lambda M^2 \leq 1/9$. It is shown by Kuhfittig [12] that

$$V''(a_0) = \frac{2}{a_0^2} \frac{-1 + 3\Lambda M^2 (a_0/M)^2 - (2/3)\Lambda M^2 (a_0/M)^3}{a_0/M - 2 - (1/3)\Lambda M^2 (a_0/M)^3} > 0. \tag{6.1}$$

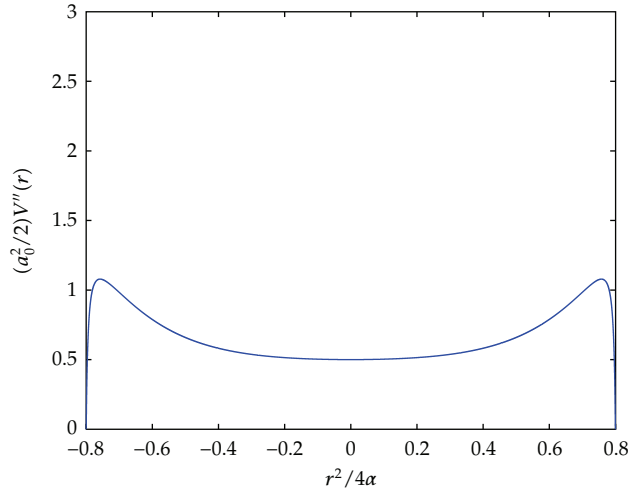

Figure 6: The de Sitter wormhole with $\Lambda M^2 = 0.045$ and $\alpha = 0.1$.

Here, V'' is a function of a_0 with ΛM^2 fixed. In the de Sitter case, the thin-shell wormhole is stable if and only if

$$1 - \frac{2}{a_0/M} - \frac{1}{3}\Lambda M^2\left(\frac{a_0}{M}\right)^2 < 0. \tag{6.2}$$

Choosing $a_0/M = 5$ (arbitrarily), we obtain $\Lambda M^2 > 0.07$, required for a stable solution. To test the smearing effect, we choose $\Lambda M^2 = 0.045$ (again subject to some uncertainty). The graph of

$$\left(\frac{a_0^2}{2}\right)V''(r) = \frac{-1 + 3(0.045)(5^2)\gamma^2 - (2/3)(0.045)(5^3)\gamma^3}{5\gamma - 2 - (1/3)(0.045)(5^3)\gamma^3} \tag{6.3}$$

is shown in Figure 6. Once again, we see a small region of stability even though ΛM^2 is much less than 0.07.

In the anti-de Sitter case ($\Lambda < 0$), the wormhole is stable whenever $a_0/M > 4.5$ and

$$\Lambda M^2 < \frac{1}{(a_0/M)\left[3(a_0/M) - (2/3)(a_0/M)^2\right]}. \tag{6.4}$$

Choosing $a_0/M = 5$ again, $\Lambda M^2 < -0.12$ for a stable solution. If we choose $\Lambda M^2 = -0.08$, thereby violating the condition, the smearing effect produces a plot for $(a_0^2/2)V''(r)$ that is similar to the graph in Figure 6.

In summary, while the wormholes in the de Sitter and anti-de Sitter spacetimes normally require sufficiently large $|\Lambda|$ to get a stable solution, a noncommutative geometry background allows much smaller values of $|\Lambda|$.

7. Conclusion

This paper reexamines a special class of thin-shell wormholes known to be unstable to linearized radial perturbations in classical general relativity (GR). In the framework of noncommutative geometry, however, small regions of stability are obtained, thereby allowing small radial perturbations. The size of the stability region depends on the parameter α, which is used to measure the degree of smearing due to the intrinsic uncertainty.

For the four spacetimes considered, regions of stability were obtained for the normally unstable Schwarzschild wormhole, for the Reissner-Nordström wormhole without requiring a naked singularity, and for both the de Sitter and anti-de Sitter wormholes for $|\Lambda|$ much smaller than the values required in a GR setting.

Acknowledgment

The author would like to thank Vance Gladney for helpful discussions.

References

[1] E. Witten, "Bound states of strings and p-branes," *Nuclear Physics B*, vol. 460, no. 2, pp. 335–350, 1996.
[2] N. Seiberg and E. Witten, "String theory and noncommutative geometry," *The Journal of High Energy Physics*, no. 09, article 32, p. 93, 1999.
[3] A. Gruppuso, "Newton's law in an effective non-commutative space-time," *Journal of Physics A*, vol. 38, no. 9, pp. 2039–2042, 2005.
[4] A. Smailagic and E. Spallucci, "Feynman path integral on the non-commutative plane," *Journal of Physics A*, vol. 36, no. 33, pp. L467–L471, 2003.
[5] P. Nicolini, A. Smailagic, and E. Spallucci, "Noncommutative geometry inspired Schwarzschild black hole," *Physics Letters B*, vol. 632, no. 4, pp. 547–551, 2006.
[6] M. Visser, "Traversable wormholes from surgically modified Schwarzschild spacetimes," *Nuclear Physics B*, vol. 328, no. 1, pp. 203–212, 1989.
[7] E. F. Eiroa, "Thin-shell wormholes with a generalized Chaplygin gas," *Physical Review D*, vol. 80, no. 4, Article ID 044033, 2009.
[8] F. S. N. Lobo and P. Crawford, "Linearized stability analysis of thin-shell wormholes with a cosmological constant," *Classical and Quantum Gravity*, vol. 21, no. 2, pp. 391–404, 2004.
[9] E. Poisson and M. Visser, "Thin-shell wormholes: linearization stability," *Physical Review D, Third Series*, vol. 52, no. 12, pp. 7318–7321, 1995.
[10] F. Rahaman, M. Kalam, and S. Chakraborty, "Thin shell wormholes in higher dimensional Einstein-Maxwell theory," *General Relativity and Gravitation*, vol. 38, no. 11, pp. 1687–1695, 2006.
[11] F. Rahaman, K. A. Rahman, S. A. Rakib, and P. K. F. Kuhfittig, "Thin-shell wormholes from regular charged black holes," *International Journal of Theoretical Physics*, vol. 49, no. 10, pp. 2364–2378, 2010.
[12] P. K. F. Kuhfittig, "The stability of thin-shell wormholes with a phantom-like equation of state," *Acta Physica Polonica B*, vol. 41, no. 9, pp. 2017–2029, 2010.
[13] F. Rahaman, P. K. F. Kuhfittig, K. Chakraborty, A. Usmani, and S. Ray, "Galactic rotation curves inspired by a noncommutative-geometry background," *General Relativity and Gravitation*, vol. 44, no. 4, pp. 905–916, 2012.